

JOINT US/JAPANESE PROGRAM OF FULL-SIZE BUILDING
TESTS FOR BASE SEISMIC ISOLATION

T. Kuroda

CONF-900804--19

Nuclear Power Division, Shimizu Corporation
Tokyo, Japan

DE90 011156

Y. W. Chang and R. W. Seidensticker

Argonne National Laboratory
Argonne, Illinois 60439, U.S.A.

ABSTRACT

Shimizu Corporation of Japan and Argonne National Laboratory of the U.S.A. initiated a joint research program on base seismic isolation. The program is centered on testing and analyzing isolation systems in a full-size building and to obtain data on relative response between isolated and non-isolated structures under earthquake conditions. The test facility consists of two identical full-size three-story buildings built side by side, located at Tohoku University in Sendai, Japan. Since April 1989, after the installation of bearings, over 20 earthquake data have been recorded at Sendai test facility. This paper describes the test facility, isolation bearings, observed earthquake records, and responses of isolated and nonisolated buildings under earthquake loads.

INTRODUCTION

Although the use of seismic isolation is growing rapidly worldwide, there exists a general lack of data on the response of isolated structures to actual earthquakes. Early in 1989 Shimizu of Japan and Argonne National Laboratory of the United States initiated a joint research program to help fill this void. The Argonne portion of the study is funded by the National Science Foundation (NSF). The program is centered on testing and analyzing isolation systems in full-size building and to obtain data on relative response between isolated and nonisolated structures. This latter feature of the program results from the unique design of the test facility, located at Tohoku University in Sendai, Japan (about 200 miles

DISCLAIMER

This report was prepared as an account of work sponsored by an agency of the United States Government. Neither the United States Government nor any agency thereof, nor any of their employees, makes any warranty, express or implied, or assumes any legal liability or responsibility for the accuracy, completeness, or usefulness of any information, apparatus, product, or process disclosed, or represents that its use would not infringe privately owned rights. Reference herein to any specific commercial product, process, or service by trade name, trademark, manufacturer, or otherwise does not necessarily constitute or imply its endorsement, recommendation, or favoring by the United States Government or any agency thereof. The views and opinions of authors expressed herein do not necessarily state or reflect those of the United States Government or any agency thereof.

DISCLAIMER

Portions of this document may be illegible in electronic image products. Images are produced from the best available original document.

buildings built side by side, except that one structure is seismically isolated and the other is not. The facility easily adapts to a variety of seismic isolation systems. Since Sendai is quite active seismically, considerable data can be obtained in a relatively short period of time.

Isolation system installed at Sendai in April 1989 has been extensively tested in the laboratory. The isolation bearings are made of high-damping rubber laminated with steel plates. They are quite similar to that proposed for the GE LMR PRISM reactor. The PRISM bearings have been tested both dynamically (at ETEC) and statically (at the EERC at the University of California, Berkeley). The project results, therefore, provide integrated sets of data ranging from individual bearing tests-to-failure to measured response of the full-size building (using these bearings) to actual earthquakes. The system response of the adjacent non-isolated building to the same earthquakes can provide valuable data for comparative purposes.

The results of the tests from this joint program are fully coordinated with the current USDOE program in seismic isolation for advanced LMR reactors. This also ensure the usefulness of the test results in demonstrating improved reliability and safety through the use of seismic isolation.

Over 20 earthquakes have been recorded at the Sendai test facility since April 1989, although none of these has been very severe. Duplicate bearings made along with those installed in the test facility have been tested both in Japan and in the United States. Results of all of these tests and events are presented and discussed below.

DESCRIPTION OF THE SENDAI BUILDINGS AND ISOLATION BEARINGS

Two test buildings, one conventionally designed and other base-isolated, were constructed side by side at Tohoku University located in Sendai, in the northern part of Japan.

The test buildings consist of two full-size, three-story reinforced concrete structures. The dimensions and construction details of the superstructure were exactly the same for both buildings. The buildings were constructed as rigid frame structures with outer walls made of light weight concrete panel. The plan dimensions of the building are 6 by 10 meters (19.685 by 32.808 ft). The total combined floor areas is 180 m^2 (1937.49 ft^2). The test buildings were completed in May 1986.¹⁻³

Figure 1 shows a general view of the test buildings. The building on the left is the ordinary one, whereas on the right is the base-isolated structure. The plan and elevation of the test structures given in Fig. 2 show six isolator bearings installed in the base-isolated building. Note from this figure that the ordinary building is surrounded by backfilled soil below the ground level and that the basement wall is made of reinforced concrete. The presence of soil embedment and concrete wall definitely will have certain mitigating effects on the building response. As for the isolated building, ample space is provided around the side of the basement wall to allow unrestricted movement of the superstructure. The base-isolation system consists of by six laminated steel-rubber bearings. The test buildings were built in a relatively hard loam layer containing gravel, whose shear wave velocity is 310 m/sec (1017 ft/sec).

The isolation system of the base isolated building consists of six identical bearings which were designed by ANL and manufactured in the U.S. This work was funded by the National Science Foundation under a joint research project between ANL and Shimizu Corporation. The bearings were installed by Shimizu of Japan in April 1989. These bearings are laminated composites with 33 alternating layers of high-damping rubber and steel plates (shims) manufactured by Fluorocarbon Inc., USA. High-damping rubber bearing is used since it seems to be well suited for applications in seismic isolation and is currently being used or proposed to be used in many structures, including buildings and nuclear facilities.

Figure 3 shows the engineering details of the elastomer bearing. The outer diameter and overall height of the bearing are 508 and 284.2 mm (20 and 11 3/16 in), respectively. The design isolation frequency of the bearings, corresponding to the 50% shear strain, is 0.75 Hz. The design value for the horizontal stiffness of each bearing is 963 Kg/cm (5382 lb/in) for the entire isolation system (6 bearings).

The dowel joint used at the top and bottom plates of the bearing transfers lateral loads from the structure to the bearing and to the foundation. The dowels are free to move vertically.

To investigate the response characteristics of the laminated bearings, the Shimizu Institute of Technology has conducted a series of static and dynamic tests on two bearings. Detailed test results, labeled as specimen No. 1 and 2, are given in Ref. 1.

To illustrate the test data, Fig. 4 presents the equivalent stiffness and damping ratio as a function of relative horizontal displacement between the top and bottom of the isolator bearing. The data were taken from test specimen Nos. 1 and 2, the static loading experiment of Tohoku

University test building, as well as data generated when Bridgestone Rubber Company bearings had been installed in the test building before the ANL tests. It is worthwhile to note that the stiffness and damping ratio obtained from the site experiment are somewhat lower than those obtained from individual bearing tests. Figure 4 also reveals that as the horizontal displacement increases, the bearing horizontal stiffness decreases. Thus, small displacement caused by minor earthquakes the isolator horizontal stiffness would be very high (much higher than the designed value of 0.75 Hz). Figure 4 indicates that for very small displacements (about 0.4 cm), the damping ratio obtained by the site experiment is about 10%. As the displacement amplitude increases, the damping ratio will first increase and then decrease to 8% at displacement of 8.5 cm. Damping ratios for displacements less than 0.4 cm are not available from either the specimen test or site experiment.

EARTHQUAKE OBSERVATION DATA

Following the installation of ANL-designed isolation bearings on April 17, 1989, 20 earthquakes were observed and their records were transmitted to ANL. Since the entire acceleration records are quite voluminous, only one representative earthquake record, i.e., record #6, is used for the discussion of relative response between isolated and nonisolated structures. For information regarding the magnitudes, distributions of epicenters, and epicentral distance of these earthquakes one should refer to Ref. 1.

RESPONSES OF ISOLATED AND NONISOLATED BUILDINGS

Three-dimensional frame models are used in numerical simulations for both convention and base-isolated buildings. In the analyses, beams, columns, and girders are all modeled by 3-D beam elements with six degrees of freedom per node to account for the translations and rotations generated from seismic events. Stiffnesses of the outer walls and partitions that are not structurally connected to the beams and girders are neglected in the calculation. However, their masses are appropriately lumped to the element nodal points, so that their inertia effects are included in the analysis.

The mathematical models of both ordinary and base-isolated buildings are given in Fig. 5. These two models are almost identical except that different modeling techniques are used for the substructure connecting the basement slab and the first floor. More specifically, major difference is in the middle portion of the support columns where the isolator is located. For the ordinary building, each basement column is represented by three beam elements in which the stiffness of the basement reinforced concrete wall is included. For the isolated building, on the other hand, the isolator is modeled by two spring elements; one linear spring and one nonlinear elastoplastic spring to simulate, respectively, the vertical and horizontal responses of the isolator. Two beam elements, similar to those columns of the superstructure are then utilized above and below the isolator to model the reinforced concrete pedestals.

To facilitate the numerical simulation, separate models are employed to analyze the horizontal responses in the transverse (X) and longitudinal (Y) directions. In these models only input accelerations at the basement

nodes and building boundary conditions are different due to differences in the direction of seismic excitation. Other input data are identical.

In calculating the horizontal response of the isolator a bilinear force-displacement constitutive equation is used for the nonlinear spring element. This relationship is determined from the dynamic tests of the ANL bearings conducted by the Shimizu Corporation.² The stiffness used in the numerical analysis is given in Fig. 6.

In addition to the stiffness, the damping ratio of the isolator is also an important parameter for the numerical simulation. The damping ratio obtained from the site experiment, corresponding to 0.4 cm (0.16 in) horizontal displacement, is about 10%, and it is lower if the relative displacement is smaller. Since the maximum isolator displacement obtained from the preliminary calculations is only 0.15 cm (0.06 in), an extrapolated damping ratio of 7.25% is thus used in the numerical simulations.

As a first step, the 3-D frame model of the ordinary building is used to study the fundamental building characteristics. Results of modal analysis revealed that the frequencies of the first two modes are 3.57 and 4.15 Hz. They correspond to the transverse (X) and longitudinal (Y) directional vibrations, respectively. The frequencies of the test building in these two directions obtained by the Shimizu Corporation of Japan are 3.63 and 4.38 Hz. The agreement of predicted and measured frequency characteristics is quite good.

Based on the 3-D models, the responses of the test buildings are investigated for records from earthquake #6, using the observed basement accelerations of the isolated building as input. The analytical results are then compared with the actual observations at locations where instrumentations are located, i.e., at the first floor and roof.

Comparisons of the calculated and observed acceleration responses for both ordinary and isolated buildings are described below.

This earthquake (i.e., #6) occurred quite near the test building on June 24, 1989. It had a magnitude of 4.4 and epicentral distance of about 6 km from the test facility. The earthquake caused the largest ground accelerations at the ground surface when compared with other earthquakes detected between April and December, 1989.

Figure 7 provides observed accelerations in the transverse (X) and longitudinal (Y) directions at the basement of the isolated building. The maximum accelerations corresponding to these two directions are 34 and 19 gal [13.11 and 7.43 in/sec²], respectively. These values are higher than those of other earthquakes. These recorded acceleration time histories were used in time-history analyses of building responses.

Since the isolation device is designed to protect the structure against strong earthquakes, the advantage of using base isolation system for earthquake #6 is thus more pronounced. We will proceed to describe the results of the comparison.

Ordinary Building

The observed and calculated transverse (X-direction) accelerations of the first floor are given in Fig. 8. Excellent comparison has been found, not only the peak values and the times of occurrence, but also the response shapes and characteristic frequencies. Figure 9 depicts the comparison of roof accelerations in the transverse (X) direction. As can be seen from these figures, both accelerations correlated very well with each other. However, the maximum accelerations differ by 28%. Such deviation may be attributed to the lack of soil-structure-interaction

treatment of the embedment of ordinary building in the numerical simulation. Also, it is noted from the analytical results that the roof vibrates with a frequency approximately 3.50 Hz, which value compares satisfactorily with the field test result of 3.63 Hz obtained by the Shimizu Corporation of Japan.

In the longitudinal (Y) direction, the recorded and simulated acceleration histories at the first floor are given in Fig. 10. Excellent comparison of the accelerations can be seen from this figure. The shape of the time histories, peak values, and frequency characteristics all closely resemble each other. Both observation and simulation indicate that the amplification of the first floor acceleration is small. Because of the relatively large ground acceleration, the first floor oscillates with a dominant frequency of 4.20 Hz which is quite different from that of the ground motion. This implies that the effect of the embedment on the response of the first floor is small.

At the roof level, the observed and calculated accelerations are presented in Fig. 11. Both figures show that major seismic events occur between 10 to 15 seconds and gradually damp out around $t = 30$ sec. Exceptionally good comparison is found for the dominant frequency at the roof level, which has a value of 4.30 Hz. This frequency value, obtained from the time-history analysis, coincides with that of the model analysis.

Isolated Building

Input accelerations for simulating the transverse (X) and longitudinal (Y) responses of the isolated buildings have been presented previously in Fig. 7. The two components of ground acceleration have a dominant frequencies of 2.53 and 2.23 Hz, respectively. Numerical simulations are

carried out with computer code through 3000 cycles of computation with a 0.01 sec constant integration step.

In the transverse direction, comparison of the recorded and simulated accelerations at the first floor is shown in Fig. 12. Good agreement again has been found from these acceleration responses. Peak accelerations especially compare well. The maximum recorded acceleration is about 39 gal (15.15 in/sec^2), almost duplicates with the simulated value of 40.45 gal (15.92 in/sec^2). Note that the floor response is dominated by a frequency of 2.07 Hz which agrees closely with the simulated frequency 2.13 Hz. This frequency corresponds to the frequency of the isolator in responding to the seismic event. Also, analytical results indicate that the 3.40 Hz building frequency has been filtered out through the use of base isolation.

Figure 13 depicts the recorded and calculated acceleration histories at the roof of the isolated building. Reasonable correlation of the acceleration pulse is also obtained although the maximum acceleration is underpredicted by about 22%.

In the longitudinal direction, the observed and calculated accelerations at the first floor and roof are compared in Figs. 14 and 15. The trends of acceleration histories at the corresponding location agree excellently, as well as the maximum accelerations. The deviations between the observed and simulated peak values are 19 and 8%, respectively, at the first floor and roof. At these two locations, the dominant frequency is found to be 2.23 Hz.

SUMMARY AND CONCLUSIONS

The data used for this benchmark test were obtained from the instrument measurements of full-size reinforced concrete structures located in Sendai, Japan. The data were derived from an actual earthquake (i.e., #6). The data are of high quality and thus can be used with confidence for validation of the seismic system response program. These recorded data are also suitable for assessing the code calculational capabilities as well as the modeling techniques used in the analysis.

In the analytical simulation, two frame models were developed for calculating the seismic responses of the ordinary and base-isolated structures, respectively. The computer acceleration responses are compared to those from observations. Also, the effect of base-isolation systems was investigated by comparing the dynamic characteristics of the base-isolated building with those of the ordinary building.

From the comparison of analytical solutions with actual recorded earthquake data, several conclusions can be drawn:

(1) The numerical solution can reproduce the general shape of the acceleration responses, both for the ordinary and base-isolated buildings. The analysis accurately predicts the peak accelerations and the times of occurrence.

(2) The analysis can accurately calculate the frequency characteristics of both ordinary and the isolated buildings. The computed frequencies of the ordinary building is about 3.50 and 4.20 Hz, respectively, in the transverse and longitudinal directions. The test building frequencies are about 3.60 and 4.35 Hz. For the isolated building, the simulated frequency is about 2.13 Hz, slightly lower than the 2.30 Hz obtained from the observation.

(3) As anticipated, the advantage of isolation system for a small earthquake is insignificant. For relatively large earthquake motion, however, such as from records of #6 earthquake, the effect of isolators in reducing the roof acceleration becomes more pronounced. For instance, for this earthquake, the computed amplification factor in the transverse direction of the isolated building is about 1.46, compared to 4.07 computed for the ordinary building.

(4) The magnitude of earthquake #6 and corresponding horizontal displacements of the isolators are still considered to be small. It did not cause uplift and overturn to occur at the Sendai isolated building. Thus, the effects of uplift, overturning, and impacts of basemats cannot be assessed and compared from the current data base. Further validation of these effects is needed when strong earthquake data becomes available on much stronger ground motions.

ACKNOWLEDGMENTS

The work performed at Argonne National Laboratory was supported by the National Science Foundation under NSF Agreement No. CES-8800871.

REFERENCES

1. T. KURODA et al., unpublished information (1989).
2. K. TAMURA, H. YAMAHARA and M. IZUMI, "Proof Tests of the Base-Isolated Building Using Full-Sized Model," Proc. Seismic, Vibration, and Shock Isolation-1988, ASME, PVP-Vol. 147, pp. 21-28.

3. T. KURODA, M. SARUTA and Y. NITTA, "Verification Studies on Base Isolation Systems by Full-Scale Buildings," Proc. Seismic, Vibration, and Shock Isolation-1989, ASME, PVP-Vol. 181, pp. 1-8.

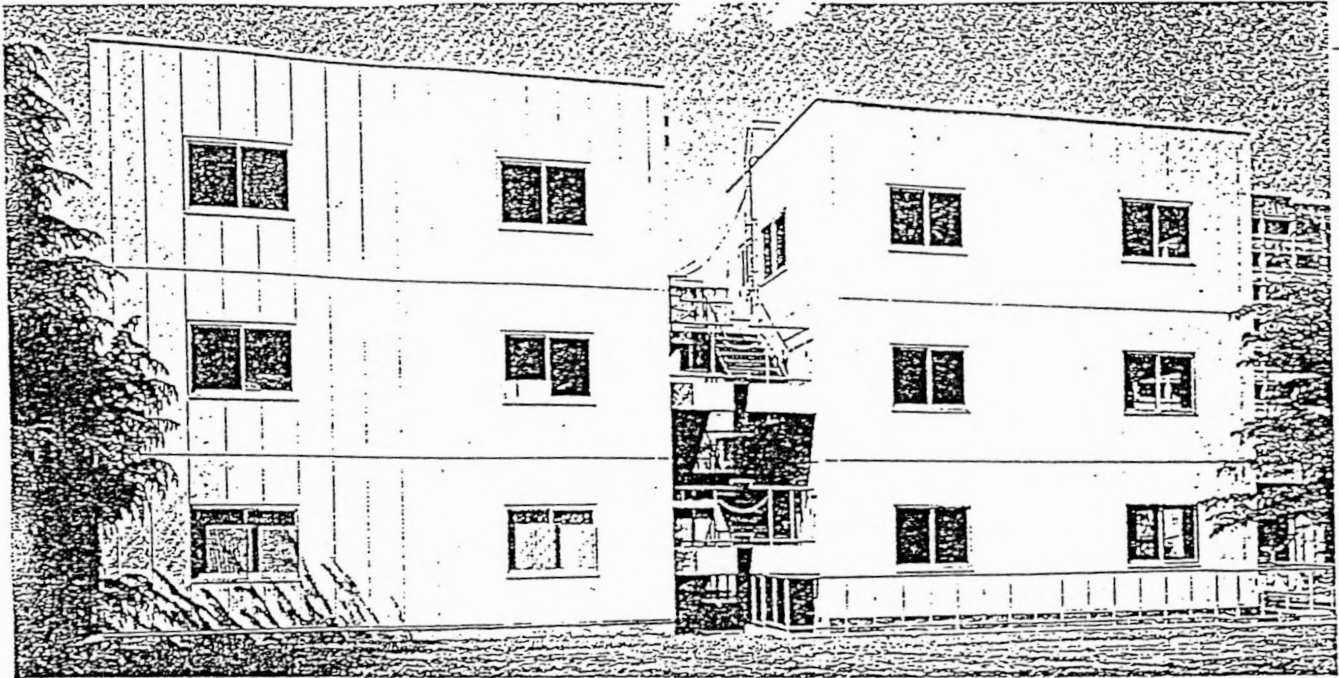


Fig. 1. General View of Test Building

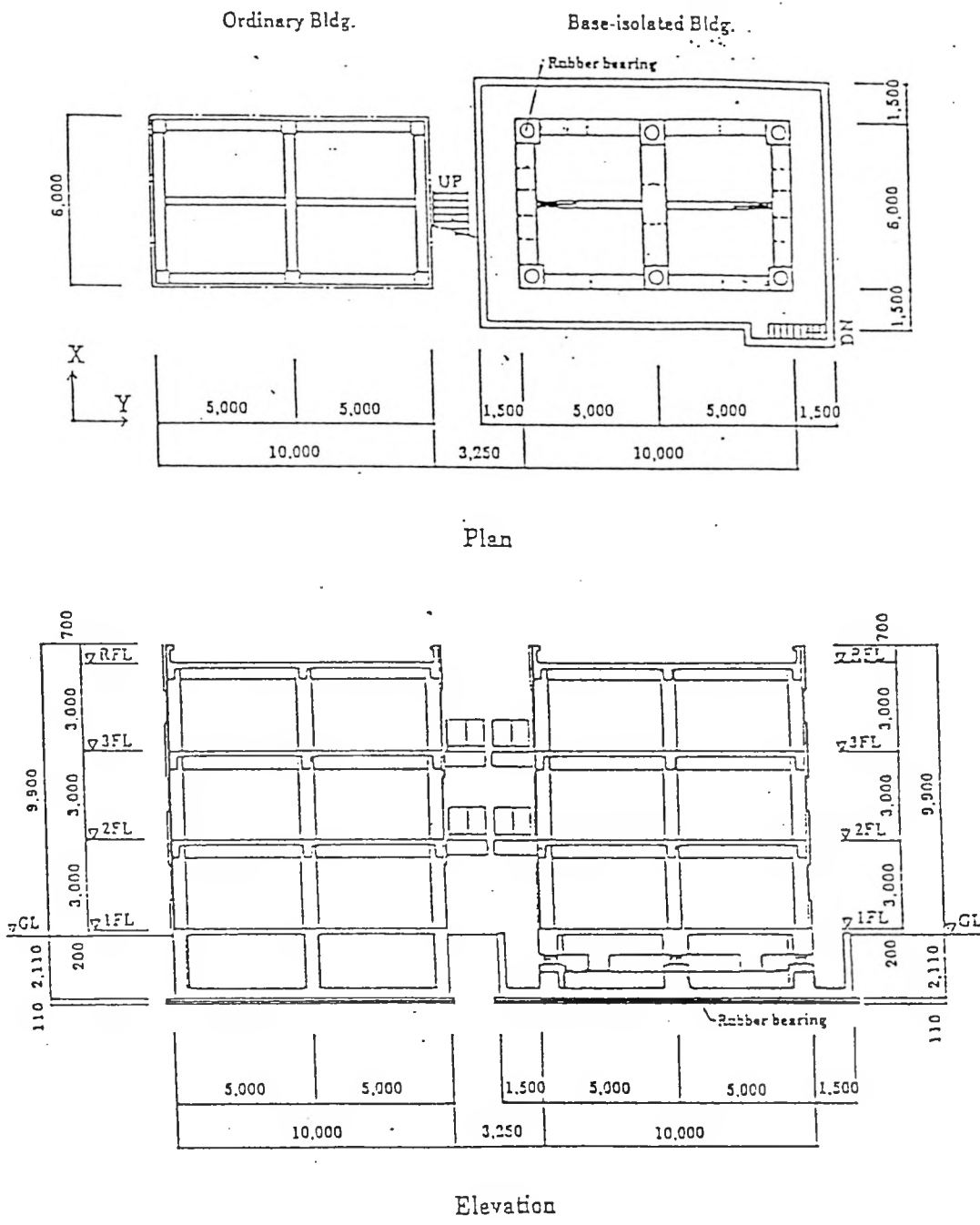


Fig. 2. Plan and Elevation Views of Test Building

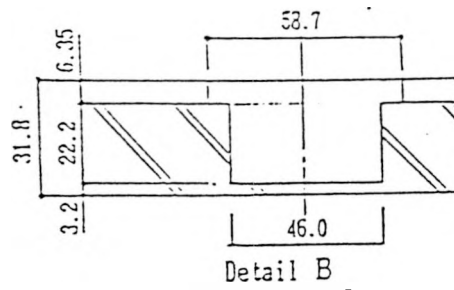
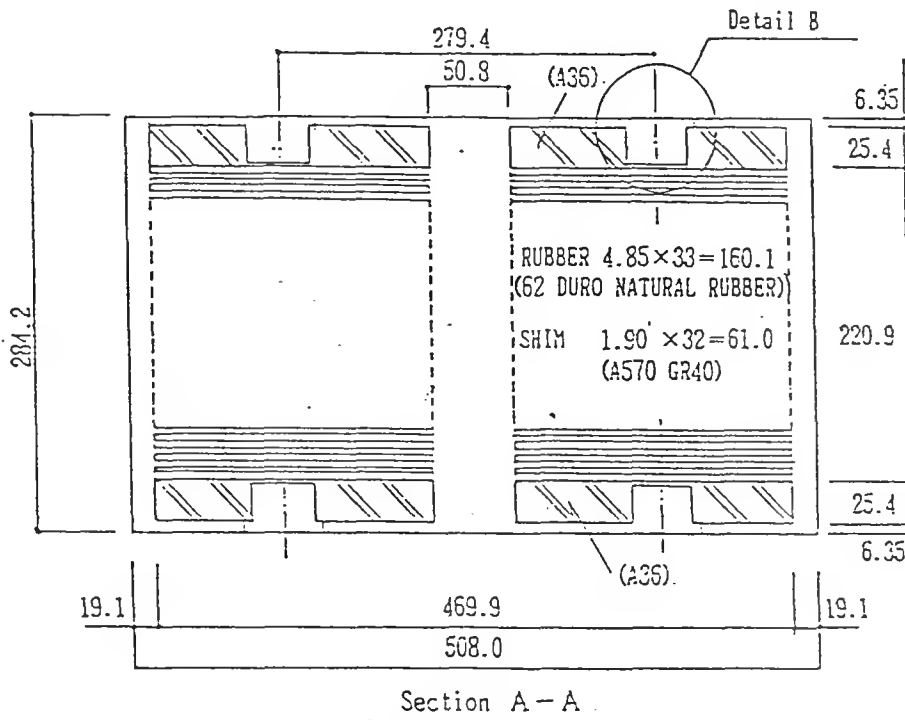
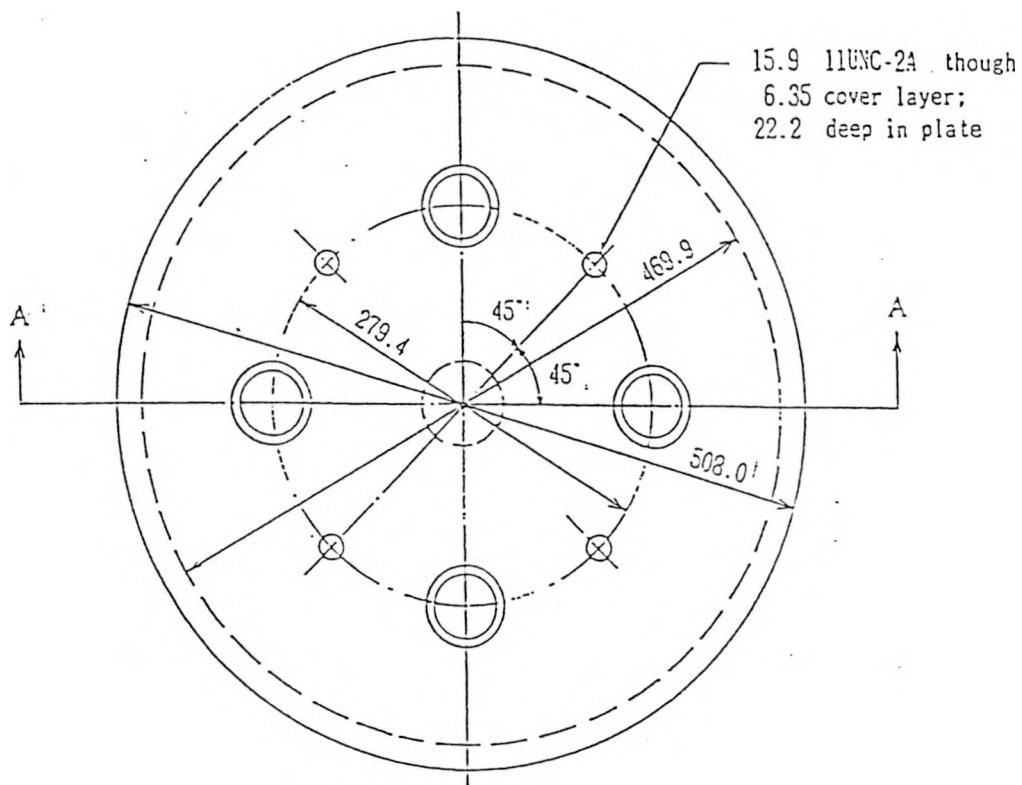


Fig. 3. Bearing Configuration and Dimensions (unit: mm)

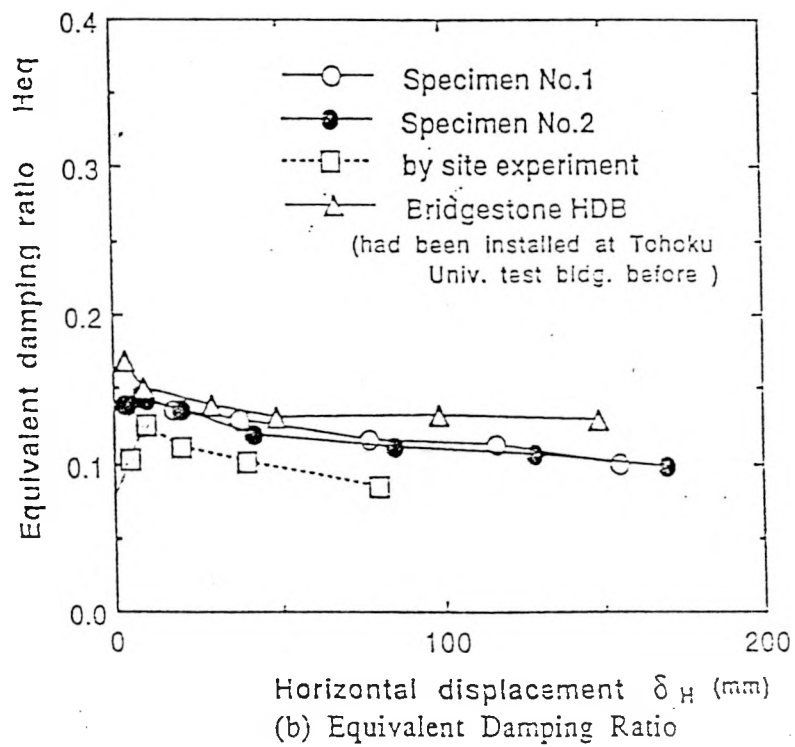
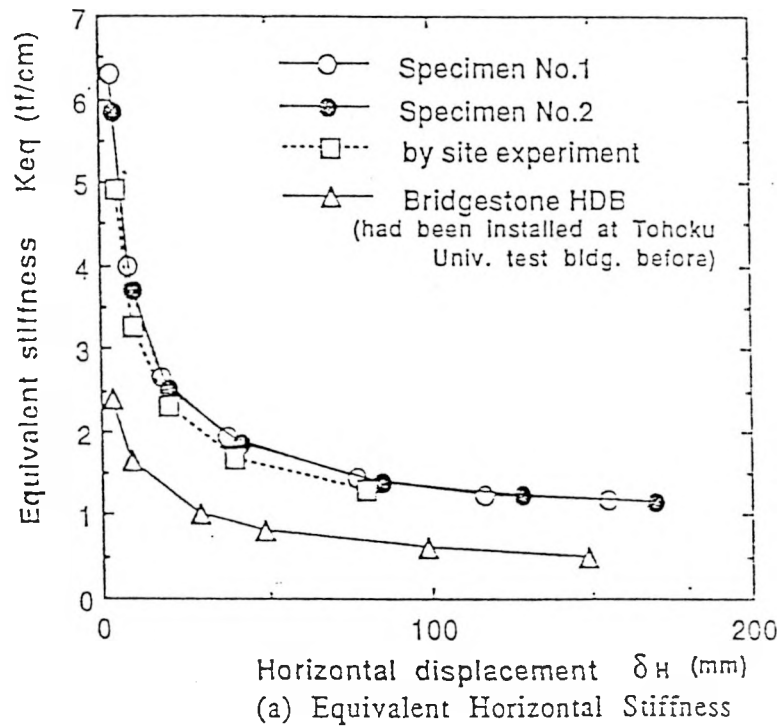
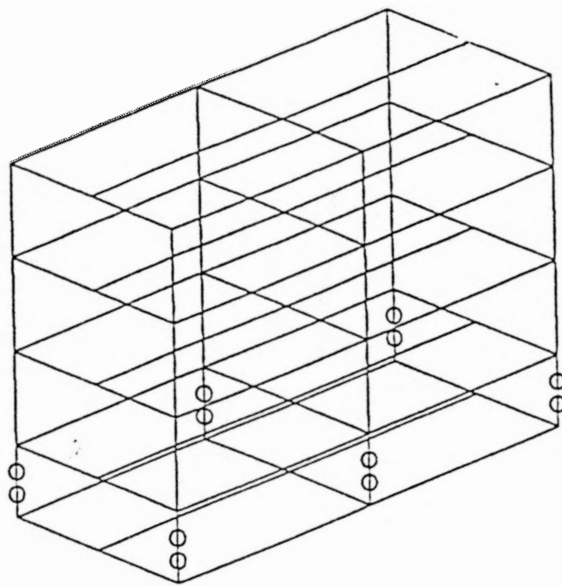
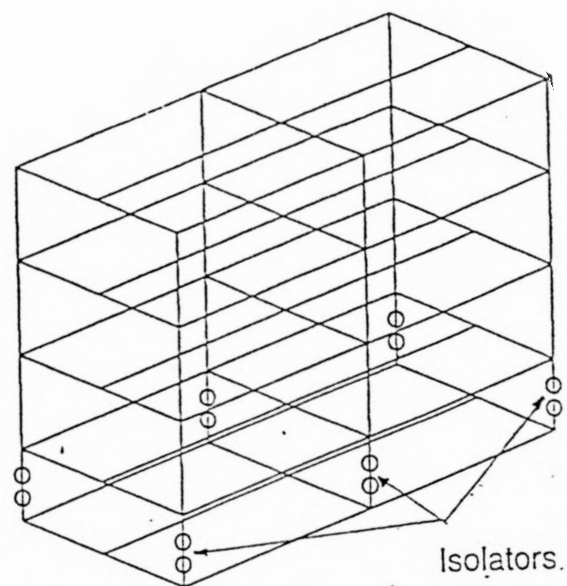


Fig. 4. Equivalent Horizontal Stiffness and Damping Ratio of Isolator

TIME = 0.000



NO ISOLATION



WITH ISOLATION

Fig. 5. Mathematical Models of Ordinary and Isolated Buildings

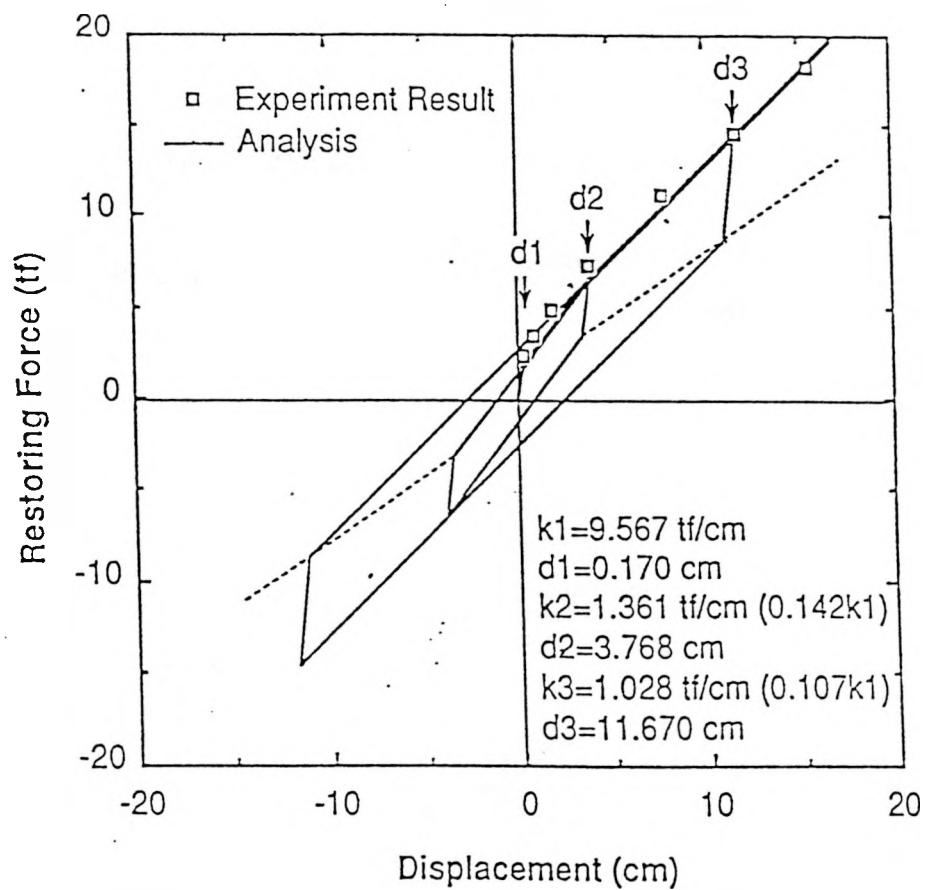
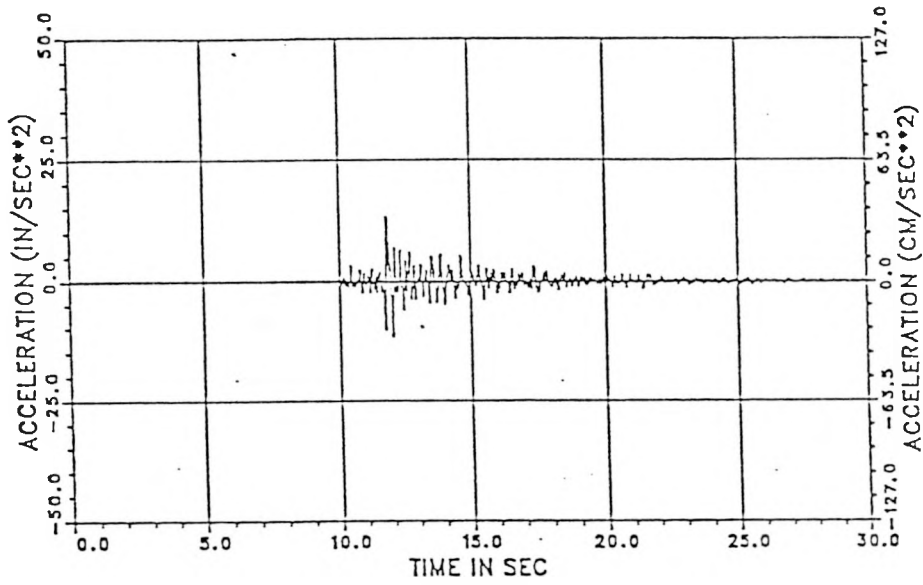


Fig. 6. Analytical Parameters for Simulating Isolator Horizontal Response

ISOL. B. - OBS. ACCEL. FILE 06 - BASE (ANL22) TRANSVERSE

TMAX,AMAX TMIN,AMIN= 11.81 13.1181 12.02 -11.6929



ISOL. B. - OBS. ACCEL. FILE 06 - BASE (ANL23) LONGITUDINAL

TMAX,AMAX TMIN,AMIN= 12.09 7.4331 11.87 -11.5512

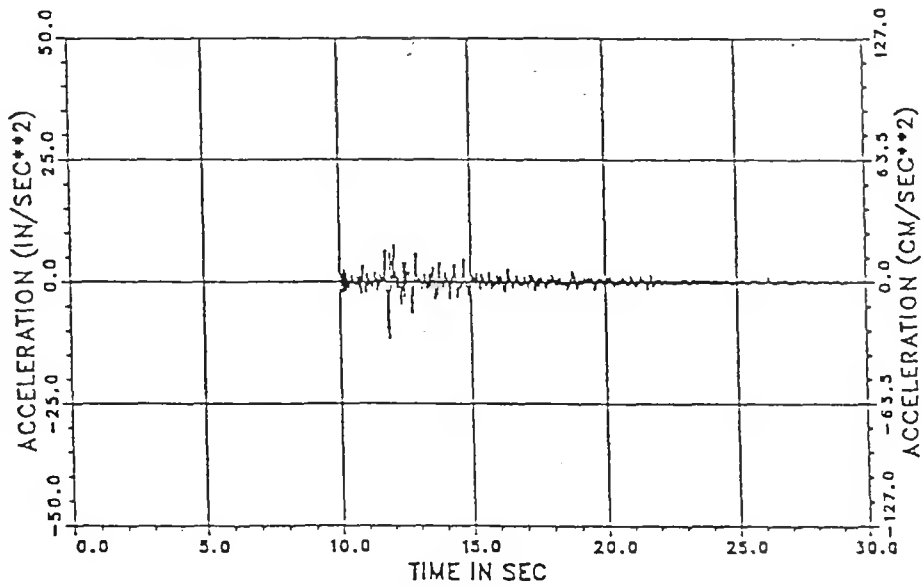
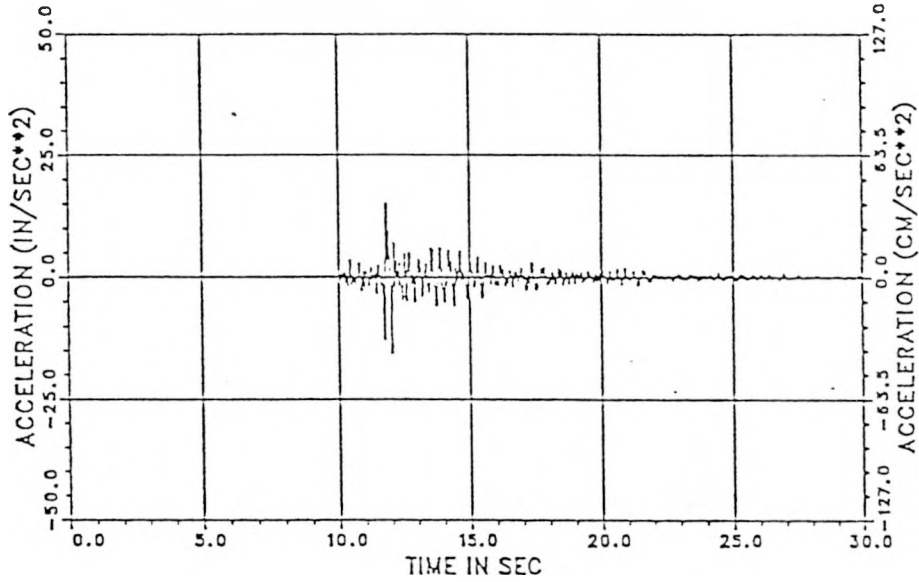


Fig. 7. Acceleration Histories Used in the SISEC Code Simulations (Top: Transverse, Bottom: Longitudinal)

ORD. B. - OBS. ACCELERATION FILE 6 - 1ST FL. (ANL17) TRANSVERSE

TMAX,AMAX TMIN,AMIN= 11.81 14.8740 12.02 -15.5236



ORD. B. - CALC. ACCEL. FILE 06 - 1ST FL. (NODE 63) TRANSVERSE

TMAX,AMAX TMIN,AMIN= 11.90 12.0781 12.04 -16.9716

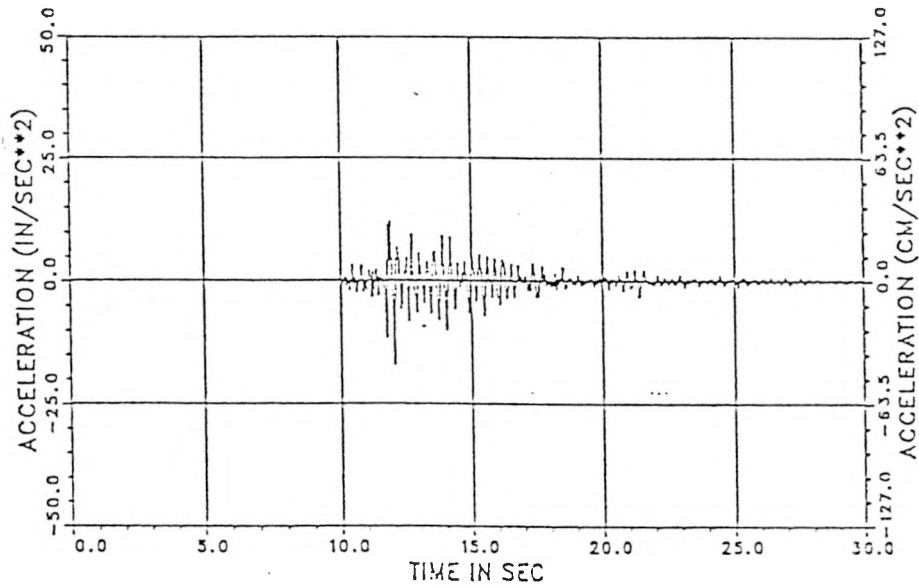
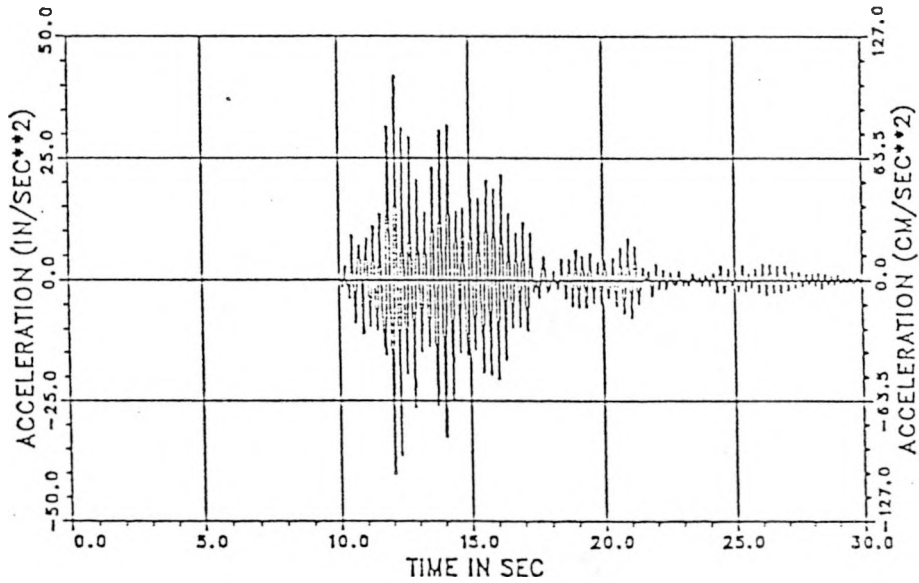


Fig. 8. Comparison of Transverse Accelerations at the First Floor of the Ordinary Building (Top: Observed, Bottom: Calculated)

ORD. B. - OBS. ACCELERATION FILE 6 - ROOF (ANL20) TRANSVERSE

TMAX,AMAX TMIN,AMIN= 12.18 41.8504 12.06 -40.2756



ORD. B. - CALC. ACCEL. FILE 06 - ROOF (NODE 9) TRANSVERSE

TMAX,AMAX TMIN,AMIN= 12.21 53.4871 12.34 -50.8515

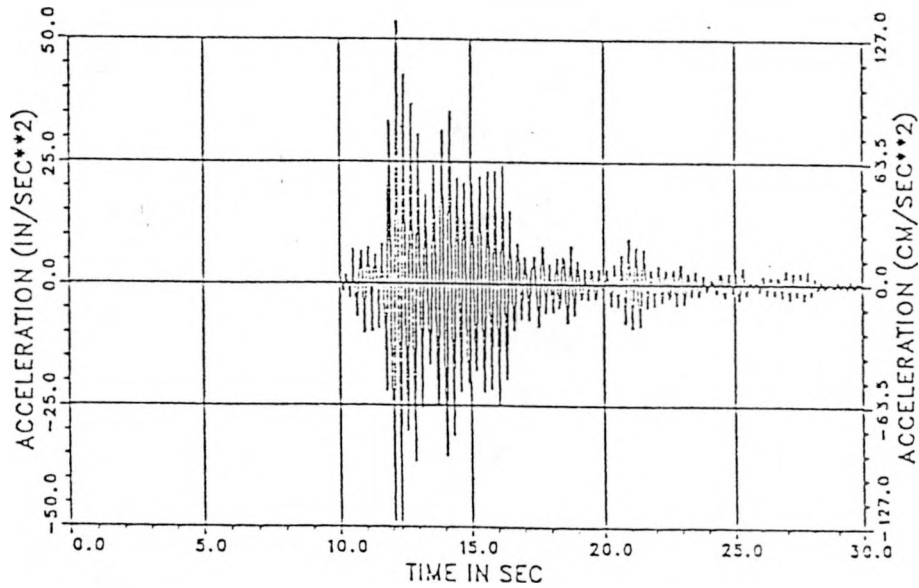
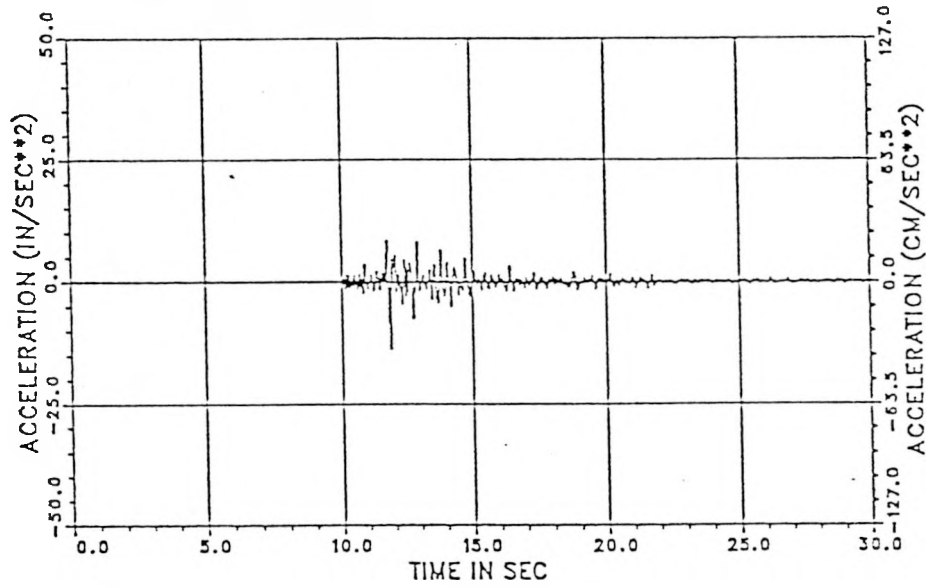


Fig. 9. Comparison of Transverse Accelerations at the Roof of the Ordinary Building (Top: Observed, Bottom: Calculated)

ORD. B. - OBS. ACCEL. FILE 6 - 1ST FL. (ANL18) LONGITUDINAL

TMAX,AMAX TMIN,AMIN= 11.76 8.2795 11.87 -13.6102



ORD. B. - CALC. ACCEL. FILE 06 - 1ST FL. (NODE 63) LONGITUDINAL

TMAX,AMAX TMIN,AMIN= 11.77 9.0192 11.89 -16.9667

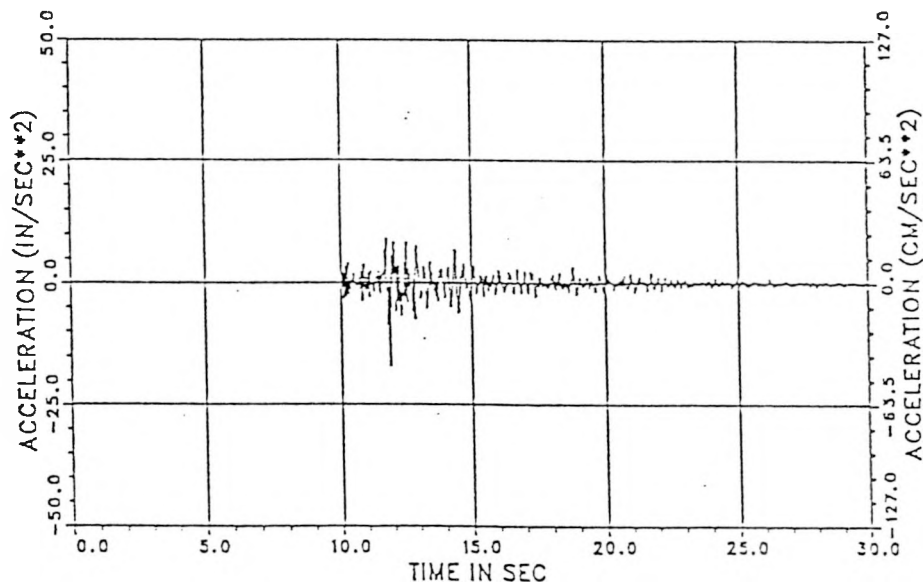
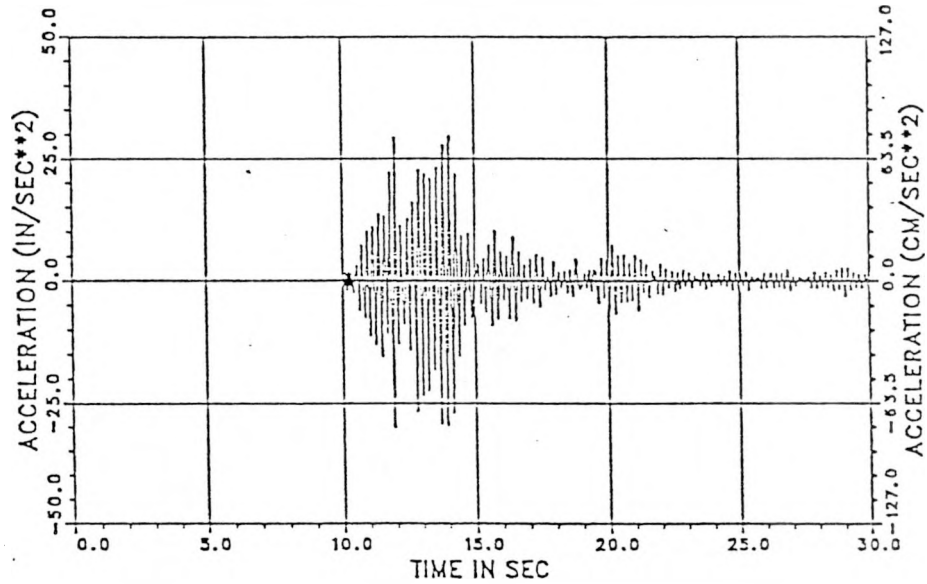


Fig. 10. Comparison of Longitudinal Accelerations at the First Floor of the Ordinary Building (Top: Observed, Bottom: Calculated)

ORD. B. - OBS. ACCELERATION FILE 6 - ROOF (ANL21) LONGITUDINAL

TMAX,AMAX TMIN,AMIN= 14.08 29.5276 11.91 -30.0512



ORD. B. - CALC. ACCEL. FILE 06 - ROOF (NODE 9) LONGITUDINAL

TMAX,AMAX TMIN,AMIN= 12.98 25.1392 13.10 -22.6359

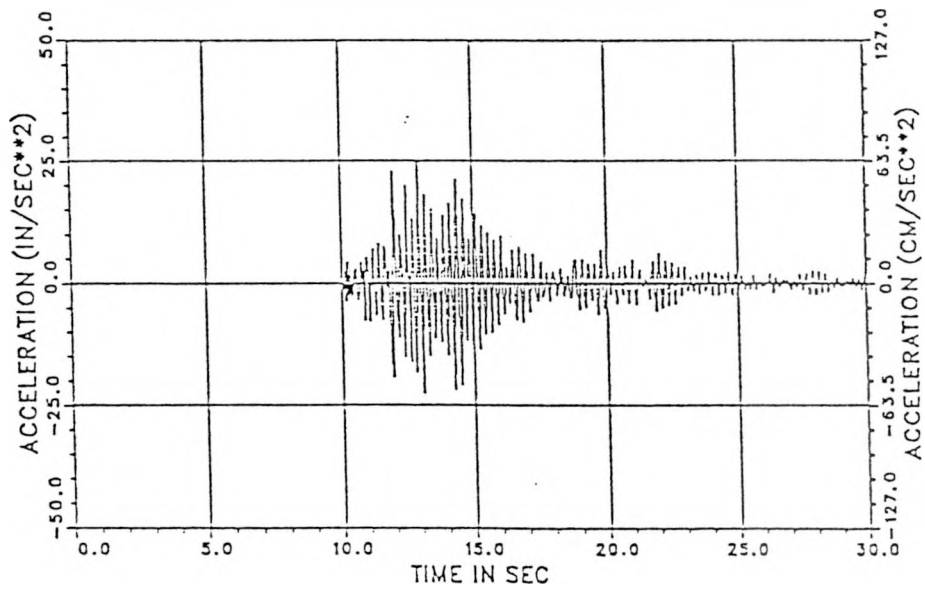
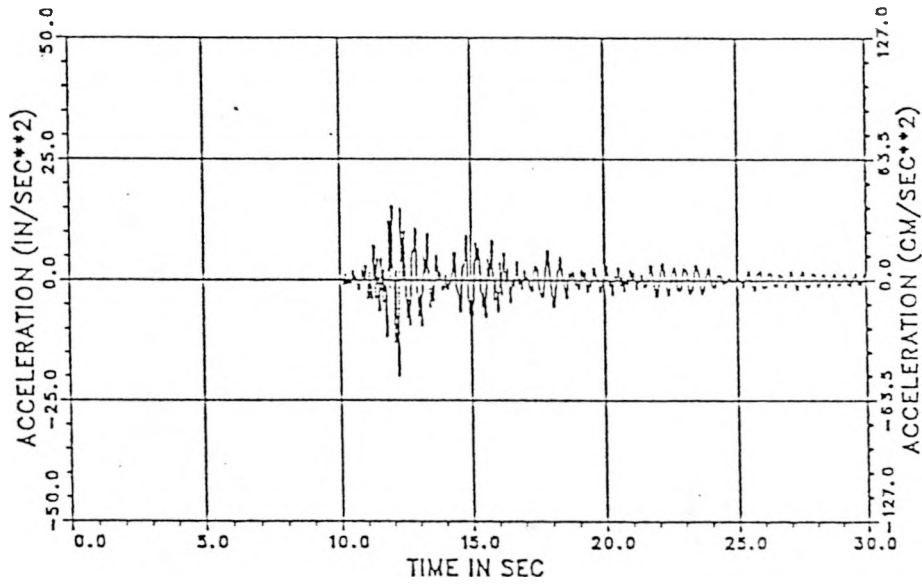


Fig. 11. Comparison of Longitudinal Accelerations at the Roof of the Ordinary Building (Top: Observed, Bottom: Calculated)

ISOL. B. - OBS. ACCEL. FILE 06 - 1ST. FL. (ANL25) TRANSVERSE

TMAX,AMAX TMIN,AMIN= 12.00 15.1457 12.23 -20.0669



ISOL. B. - CALC. ACCEL. FILE 06 - 1ST FL. (NODE 63) TRANSV.

TMAX,AMAX TMIN,AMIN= 11.97 15.9279 12.19 -16.5387

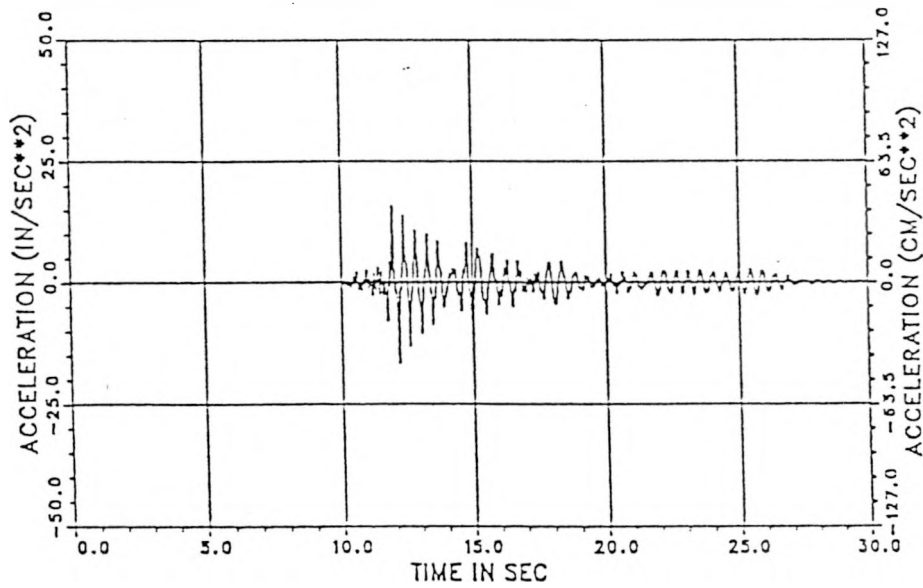
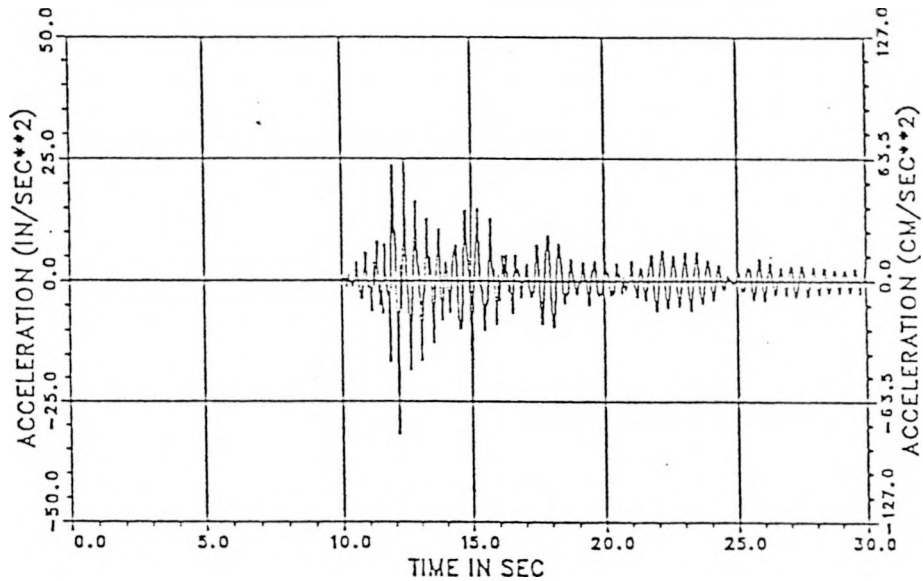


Fig. 12. Comparison of Transverse Accelerations at the First Floor of the Isolated Building (Top: Observed, Bottom: Calculated)

ISOL. B. - OBS. ACCEL. FILE 06 - ROOF (ANL30) TRANSVERSE

TMAX,AMAX TMIN,AMIN= 12.41 24.7087 12.16 -31.8819



ISOL. B. - CALC. ACCEL. FILE 06 - ROOF (NODE 9) TRANSV.

TMAX,AMAX TMIN,AMIN= 12.02 19.2637 12.13 -20.5181

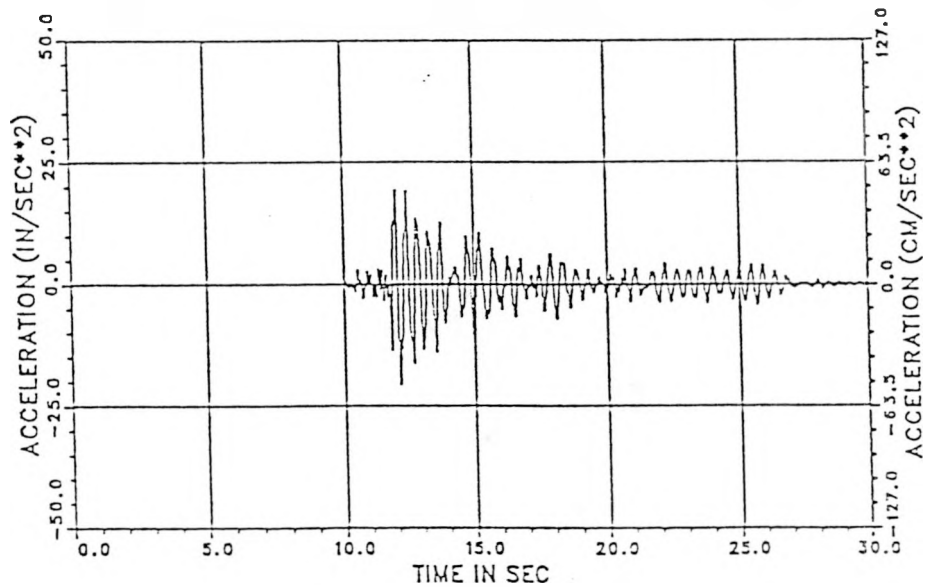
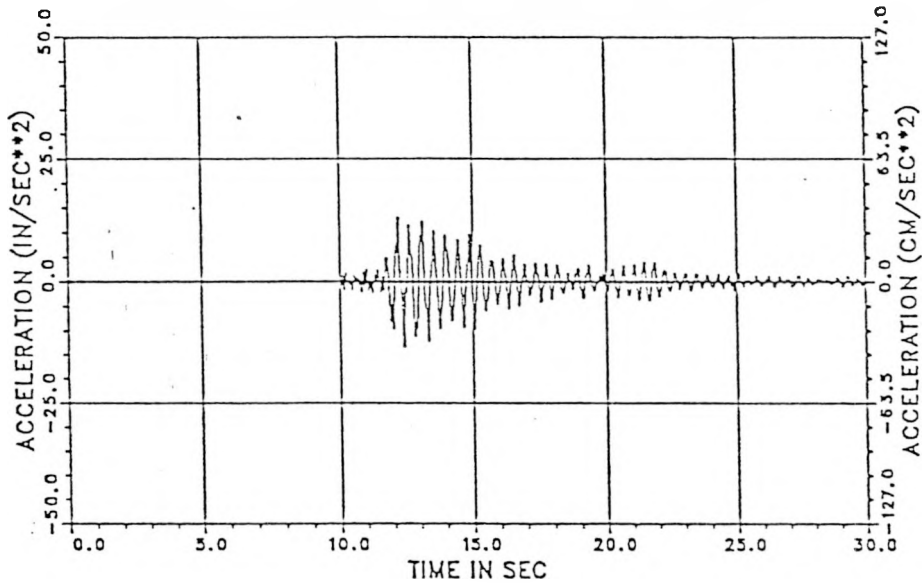


Fig. 13. Comparison of Transverse Accelerations at the Roof of the Isolated Building (Top: Observed, Bottom: Calculated)

ISOL. B. - OBS. ACCEL. FILE 06 - 1ST. FL. (ANL26) LONGITUDINAL

TMAX,AMAX TMIN,AMIN= 12.21 12.9685 12.41 -13.3780



ISOL. B. - CALC. ACCEL. FILE 06 - 1ST FL. (NODE 63) LONGITUD.

TMAX,AMAX TMIN,AMIN= 13.08 15.4663 12.88 -16.4391

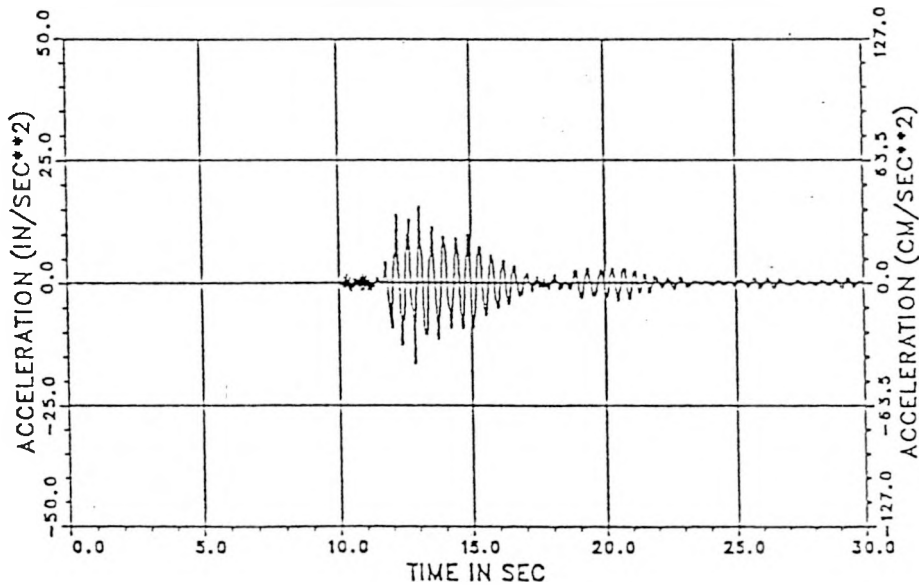
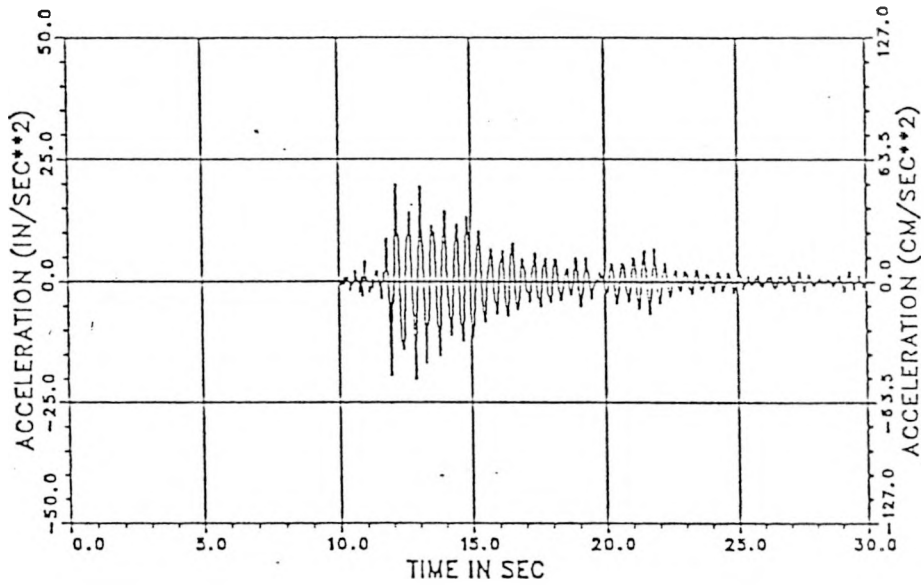


Fig. 14. Comparison of Longitudinal Accelerations at the First Floor of the Isolated Building (Top: Observed, Bottom: Calculated)

ISOL. B. - OBS. ACCEL. FILE 06 - ROOF (ANL31) LONGITUDINAL

TMAX,AMAX TMIN,AMIN= 12.16 19.8465 12.88 -20.1850



ISOL. B. - CALC. ACCEL. FILE 06 - ROOF (NODE 9) LONGITUD.

TMAX,AMAX TMIN,AMIN= 13.12 18.1061 12.44 -17.1504

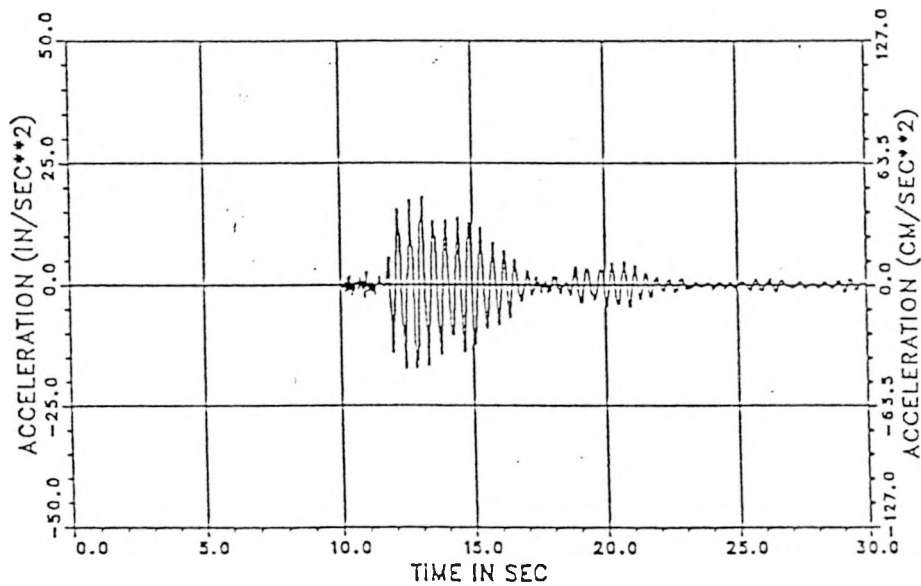


Fig. 15. Comparison of Longitudinal Accelerations at the Roof of the Isolated Building (Top: Observed, Bottom: Calculated)